Journal of The Electrochemical Society, **157** (2) F30-F34 (2010)
0013-4651/2009/157(2)/F30/5/$28.00 © The Electrochemical Society

n-Type TiO_2 Thin Films for Electrochemical Ozone Production

Kenta Kitsuka,[a,b] Kazuhiro Kaneda,[a] Mineo Ikematsu,[a] Masahiro Iseki,[a] Katsuhiko Mushiake,[a] and Takeo Ohsaka[b,*,z]

[a]*Sanyo Electric Company, Limited, ECO Technology Research Center, Gunma 370-0596, Japan*
[b]*Department of Electronic Chemistry, Interdisciplinary Graduate School of Science and Engineering, Tokyo Institute of Technology, Yokohama 226-8502, Japan*

An electrode for the electrochemical production of ozone, which has the compositional sequence $Si/TiO_x/Pt/TiO_2$ (TiO_x is titanium oxide), was fabricated by sputtering TiO_2 thin film (the thickness is typically 300 nm) on a $Si/TiO_x/Pt$ substrate. The TiO_2 thin film was characterized by X-ray diffraction, transmission electron microscopy, UV photoelectron spectroscopy, UV-visible spectroscopy, and photoelectrochemical measurements: It is an n-type semiconductor of the rutile-type TiO_2. The electrochemical ozone production (EOP) was realized, and a high current efficiency of 9% was achieved at a low current density of 8.9 mA cm^{-2} in 0.01 M $HClO_4$ at 15°C. The observed high efficiency of EOP was considered to originate from the electrocatalysis of the n-type TiO_2 in the dark when a large anodic bias was applied in which, based on the band structure of the n-type $TiO_2/HClO_4$ solution interface, electron tunneling can take place through a deep depletion layer of the TiO_2 surface.
 [DOI: 10.1149/1.3265469]

Manuscript submitted August 13, 2009; revised manuscript received October 19, 2009. Published December 9, 2009.

Ozone is a powerful oxidizing agent with a broad range of applications, and the use of ozone in aqueous solutions is of particular importance because of its environmentally friendly decomposition via a free radical chain mechanism to yield O_2. Electrochemical ozone production (EOP) has been studied extensively[1-17] for several green applications in various industries including the chemical, water treatment, pulp, food, and medical industries. The ozone production reaction at the anode by water electrolysis can be expressed as

$$3H_2O = O_3 + 6H^+ + 6e^- \quad E^\circ = 1.51 \text{ V} \qquad [1]$$

This reaction occurs at a higher potential than the oxygen evolution reaction (OER) (E° = 1.23 V). Consequently, for efficient EOP, the competition between the O_2 and O_3 formation should be shifted in favor of O_3, thereby suppressing the O_2 evolution at a reasonable current. This can be achieved using a suitable material, which is required to possess a high overpotential for the OER. Lead dioxide (PbO_2) electrode was the best candidate for EOP,[3,4,18] and a current efficiency of 6–7% for ozone production using a phosphate buffer was reported.[7] However, the use of lead-containing materials for EOP, e.g., for water sterilization, is not recommended because of the dissolution of poisonous lead species. Several papers have been published for exploring the use of alternative materials for the EOP that may meet a high overpotential for OER and that are nonpoisonous as electrodes for EOP, such as Pt[2-4] and boron-doped diamond (BDD),[8,9] together with various electrolyte solutions. Pt has the highest oxygen overpotential among the noble metals and their alloys, but it does not necessarily have a high ozone production efficiency (e.g., less than 2% at a current density of 400 mA cm^{-2}).[4] Being a p-type semiconductor, BDD has a wide electrochemical potential window and also a high oxygen overpotential.[8,9] However, it is not widely used in EOP due to its high cost and/or low ozone production efficiency at low current densities.

Recently, our group has found an excellent catalysis of tantalum oxide (TaO_x) insulator thin films, which were deposited on a Si/Pt substrate using the radio-frequency (rf) sputtering method, for the ozone production in model tap water[13] and 0.1 M perchloric acid ($HClO_4$),[14] in which its high oxygen overpotential was found to originate from the TaO_x band structure and a high current efficiency for ozone production (8% at 10 mA cm^{-2}) was achieved. The obtained current efficiency is among the highest values at room temperature, and therefore TaO_x thin film is one of the promising electrode materials for EOP. Furthermore, we have found a superior electrocatalysis of low priced titanium oxide thin film electrodes ($Si/TiO_x/Pt/TiO_x$) fabricated by spin coating on a $Si/TiO_x/Pt$ (TiO_x is titanium oxide) substrate for EOP and have reported the preliminary results on the EOP.[15,16] The influence of several factors including the electrode annealing temperature, the electrolyte composition, and the electrolysis current density on the efficiency of ozone production was investigated. A maximum ozone production efficiency of 2.5% at 74 mA cm^{-2} was obtained at room temperature. However, in this case, the Pt substrate also functioned as an electrode surface because of its partial exposure to the electrolyte solution. This is because the TiO_x thin film does not completely cover the Pt substrate, and thus the electrolyte solution reaches its surface. Therefore, it was impossible to clarify the essential role of TiO_x thin film itself in the EOP and the EOP mechanism.

Sputtering is one of the most utilized methods for obtaining uniform and dense TiO_2 thin film with a well-controlled stoichiometry among a variety of methods used to prepare TiO_2 thin films. Therefore, in this study, we employed a sputtering method to prepare a uniform and dense TiO_2 thin film on the $Si/TiO_x/Pt$ substrate. The electrochemical and photoelectrochemical properties, the band position, and the EOP activity of the TiO_2 thin film prepared were investigated in detail. Moreover, the observed high efficiency of the EOP is successfully explained based on the band structure of the n-type $TiO_2/HClO_4$ solution interface.

Experimental

Preparation of the $Si/TiO_x/Pt/TiO_2$ electrode.— Figure 1 shows the cross-sectional structure of the fabricated electrode. A Si substrate was placed inside the chamber of the rf sputtering unit (ULVAC, Inc.), and a TiO_x film was deposited onto the Si substrate. The TiO_x layer acts as a binding agent between the Si substrate and the subsequent Pt layer, increasing the durability of the electrode. It also suppresses the mutual diffusion of the Si and Pt layers. The Pt layer was deposited onto the TiO_x film (previously deposited on the Si substrate) by sputtering. Then, a metallic Ti thin film was deposited on the Pt film (previously deposited on Si/TiO_x) for 36 min at room temperature under an Ar gas pressure of 0.67 Pa and an rf power of 100 W. Finally, the Ti thin film of the thus-prepared $Si/TiO_x/Pt/Ti$ electrode was annealed at 600°C for 30 min in air. The fabricated $Si/TiO_x/Pt/TiO_2$ was set on the Ti substrate, and the Pt layer of the $Si/TiO_x/Pt/TiO_2$ was electrically connected with the Ti substrate using a Ag conducting paste. Then, the surface of the TiO_2 thin film was covered with a fluorine resin insulating tape, leaving a geometric area of 2.25 cm^2 (1.5 × 1.5 cm) exposed.

Ozone production.— A cell separated by a cation-exchange membrane (Nafion) was used to evaluate the ozone production by water electrolysis. A 0.01 M perchloric acid solution ($HClO_4$) was used as the electrolyte solution, and the solution temperature was

* Electrochemical Society Active Member.
z E-mail: ohsaka@echem.titech.ac.jp

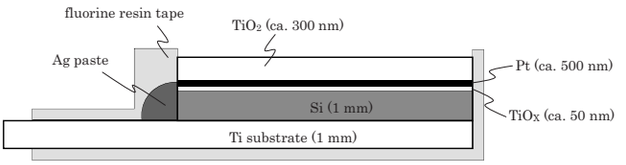

Figure 1. Cross-sectional structure of the $Si/TiO_x/Pt/TiO_2$ electrode.

maintained at 15°C. A Pt plate was used as the cathode and the $Si/TiO_x/Pt/TiO_2$ as the anode, and the distance between the anode and the cathode was maintained constant (1 cm). Constant-current electrolysis was performed for 1 min, in which the current was changed in the range of 20–120 mA (the current densities were 8.9–53.3 mA cm^{-2}). The concentration of ozone, which was electrogenerated and partitioned in the electrolyte solution phase was measured by a colorimeter (DR/4000U, HACH), and the amount of ozone gas partitioned in the gas phase (i.e., liberated from the electrolyzed solution) was not determined. Therefore, "the current efficiency for EOP" used in this study based on the amount of ozone partitioned in the electrolyte solution. The error introduced by ignoring the gas phase ozone in the estimation of the EOP current efficiency was determined to be less than 0.5%.

Characterization of the TiO_2 thin film.— The crystal structure of the TiO_2 thin film was determined by grazing incidence X-ray diffraction (XRD) operated with Cu Kα (λ = 1.54056 Å) radiation at 16.2 kW (D8-DISCOVER, Bruker AXS). A transmission electron microscope (TEM) was operated at 200 keV to observe the cross section of the TiO_2 thin film (JEM-2100F, JEOL). The UV-visible spectrum of the TiO_2 thin film surface was obtained using a thin-film metrology system (Filmtek 3000, SCI, Inc.). Ultraviolet photoelectron spectroscopy (UPS) using He(I) (21.2 eV) with a negative bias voltage (−10.0 V) was applied to the TiO_2 thin film to increase the sensitivity in the region of the lower binding energy. The spectra were calibrated with respect to the Fermi edge of Au. $Si/TiO_x/Pt/TiO_2$ was annealed at 200°C for 60 min in air to remove surface impurities before UPS measurements. The Fermi level (E_F) of the TiO_2 thin film was determined by the upper emission onset energy of the photoelectrons from Au, which was deposited on a part of $Si/TiO_x/Pt/TiO_2$.

Electrochemical and photoelectrochemical measurements.— Cyclic voltammetry and photoelectrochemical current–voltage measurements were performed in a conventional three-electrode cell using a potentiostat/galvanostat (HZ-3000, Hokuto Denko) at 24°C. The counter and reference electrodes were a platinum mesh and Ag/AgCl [saturated (sat) KCl], respectively, and the electrolyte solution (0.1 M $HClO_4$, pH 1.0) was saturated with N_2 gas before each electrochemical measurement.

For the photoelectrochemical measurements, a quartz cell was used, and the working electrode was illuminated by a 350 W Xe lamp (L2483, Hamamatsu Photonics) with wavelengths from 185 to 2000 nm. The Ag/AgCl (sat KCl) reference electrode was shielded to prevent the UV-visible irradiation.

Results and Discussion

Electrochemical ozone production.— Figure 2 shows the variation in the concentration of the electrogenerated O_3 and the current efficiency for the EOP depending on the current density from 8.9 to 53.3 mA cm^{-2}. The concentration of O_3 increases almost proportionally with increasing current density. Using Eq. 1 for the EOP, the current efficiencies were calculated: The values of 7–9% were achieved in the current density range examined, especially 9% at the low current density of 8.9 mA cm^{-2}. This high current efficiency could be achieved at a much lower current density compared with the cases (typically at 23–2000 mA cm^{-2}) using conventional electrodes for the EOP, i.e., Pt,[4,17] BDD,[8,9] and PbO_2.[3-7,18]

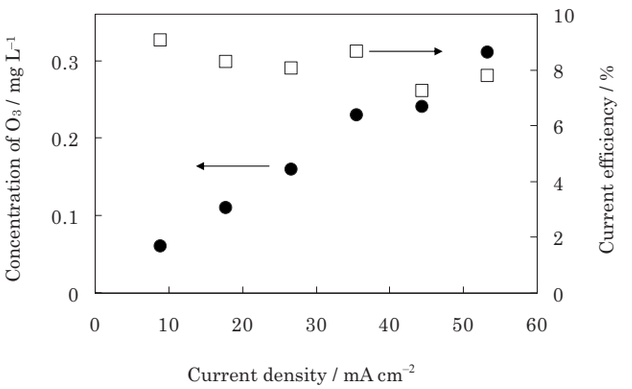

Figure 2. Current density dependence of the concentration of generated O_3 and the current efficiency for O_3 production using the $Si/TiO_x/Pt/TiO_2$ electrode. Electrolysis was performed for 1 min in 0.01 M $HClO_4$ at 15°C.

Electrochemical and photoelectrochemical measurements.— The cyclic voltammograms shown in Fig. 3 were obtained from the (a) $Si/TiO_x/Pt$ and (b) $Si/TiO_x/Pt/TiO_2$ electrodes in the potential range of −0.2 to 1.5 V vs Ag/AgCl (sat KCl) at a scan rate of 50 mV s^{-1}. In voltammogram (a), the typical cyclic voltammetry (CV) response characteristics of a Pt electrode is shown: the Pt oxide layer formation ($E > 0.6$ V) and its reduction as the cathodic peak at 0.5 V, the double-layer region ($0.1 < E < 0.5$ V), and the hydrogen adsorption/desorption ($-0.15 < E < 0$ V). However, as shown in voltammogram (b), the CV characteristics expected for the Pt electrode could not be observed at the $Si/TiO_x/Pt/TiO_2$ electrode. This result strongly demonstrates that the TiO_2 thin film completely covers the Pt surface of the $Si/TiO_x/Pt$ substrate. In addition, together with the EOP results shown in Fig. 2, it is suggested that the EOP and OER may take place on the TiO_2 thin film of $Si/TiO_x/Pt/TiO_2$. At the same time, we can see that the TiO_2 thin film exhibits an excellent "activity" for the EOP, as demonstrated by the high current efficiency compared with the conventional electrode materials used for EOP. The EOP mechanism on the TiO_2 thin-film electrode is discussed below based on the band structure of the n-type TiO_2/solution interface.

Figure 4 shows the photocurrent–voltage curves obtained from the $Si/TiO_x/Pt/TiO_2$ electrode under a chopped light irradiation from a Xe lamp in the potential range of –0.2 to 0.6 V vs Ag/AgCl (sat KCl) in 0.1 M $HClO_4$ solution (pH 1.0). The anodic photocurrent associated with water oxidation was observed under the illumination, and it increased by increasing the polarization to the positive

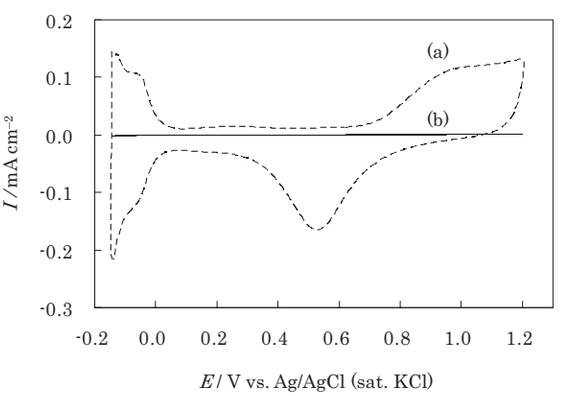

Figure 3. Cyclic voltammograms obtained from the (a) $Si/TiO_x/Pt$ and (b) $Si/TiO_x/Pt/TiO_2$ electrodes in 0.1 M $HClO_4$ solution under N_2 atmosphere at 24°C. Potential scan rate: 50 mV s^{-1}.

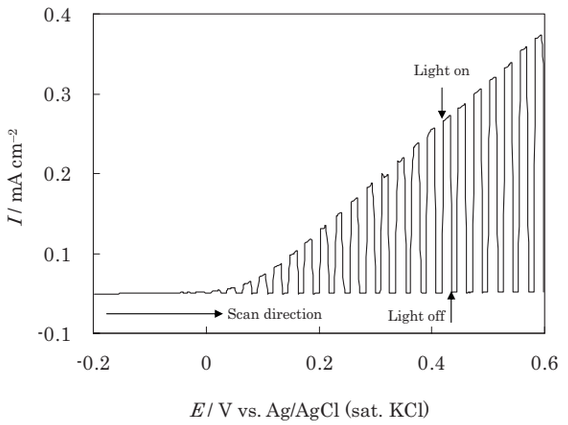

Figure 4. Current–voltage curves for the Si/TiO_x/Pt/TiO_2 electrode under an intermittent UV-visible irradiation in 0.1 M $HClO_4$. Potential scan rate: 5 mV s^{-1}.

direction of the potential, while only a very small current was observed in the dark. This result indicates that the TiO_2 thin film functions as an n-type semiconductor electrode.[19]

Characterization and UV-visible spectroscopy of the TiO_2 surface.— The XRD patterns of the Si/TiO_x/Pt/TiO_2 are shown in Fig. 5. The origin of each peak is also shown in the figure. All the diffraction peaks indicated by the symbol ● are assigned to rutile TiO_2,[20] and the other peaks (○) are characteristic of the substrate Pt.[21]

Figure 6 shows the TEM images of the cross section of the TiO_2 thin film. In Fig. 6a, a typical image of the TiO_2 thin-film structure is observed. The TiO_2 film thickness is relatively uniform and is estimated to be 300 nm. The electron diffraction analysis indicated that the film on the Pt layer is crystallized titanium oxide (i.e., rutile TiO_2). Figure 6b shows a typical high magnification image. The TiO_2 film is dense without apertures. These TEM observations support the CV response (Fig. 3b) and the EOP results (Fig. 2) obtained from the Si/TiO_x/Pt/TiO_2 electrode in 0.1 M $HClO_4$ solution; that is, the TiO_2 thin film completely covers the Pt surface, and thus no CV response characteristic of a Pt electrode is observed, but the TiO_2 thin film can effectively function as an electrode for EOP.

A typical UV-visible absorbance spectrum of the TiO_2 thin film surface of the Si/TiO_x/Pt/TiO_2 electrode in the range of 240–800 nm is presented in Fig. 7. The increase in the absorbance at shorter wavelengths is associated with the optical bandgap (E_{bg}) of the TiO_2 thin film, and its absorbance edge (λ) is estimated to be 375 nm. The E_{bg} value is calculated to be 3.3 eV by using the relationship

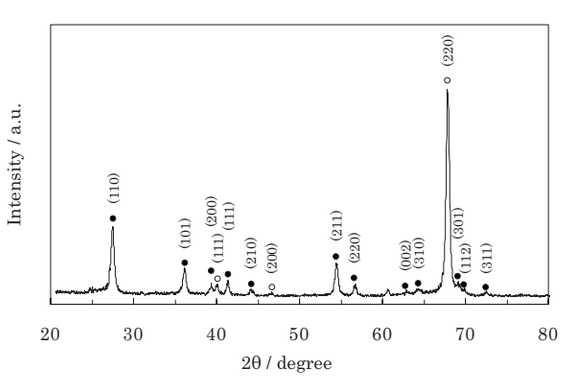

Figure 5. XRD patterns of Si/TiO_x/Pt/TiO_2. Symbols ● and ○ represent the rutile TiO_2 and Pt peaks, respectively.

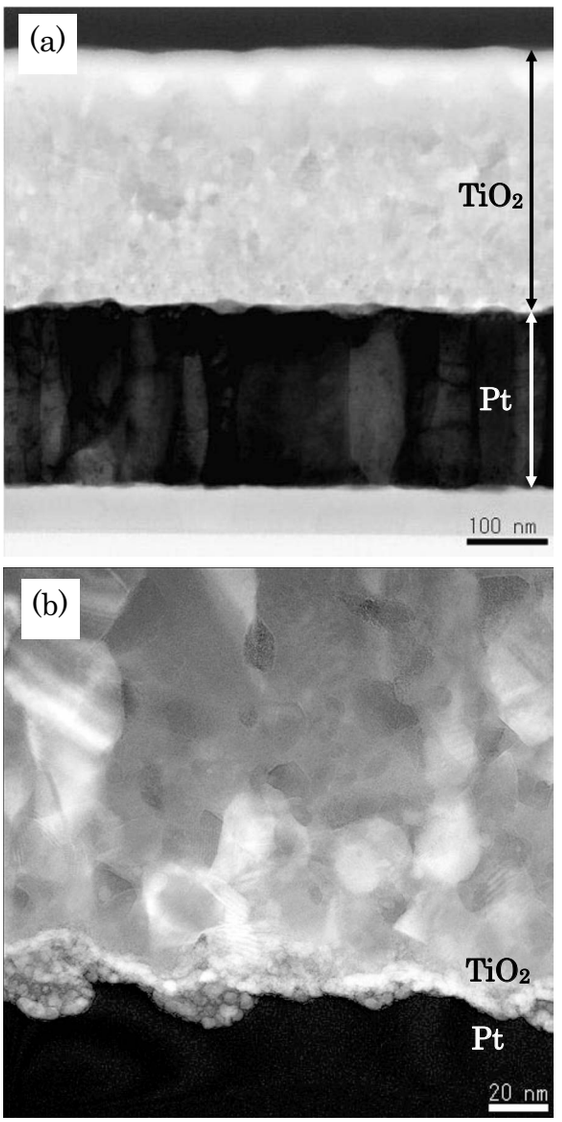

Figure 6. TEM images of the cross sections of TiO_2 thin films.

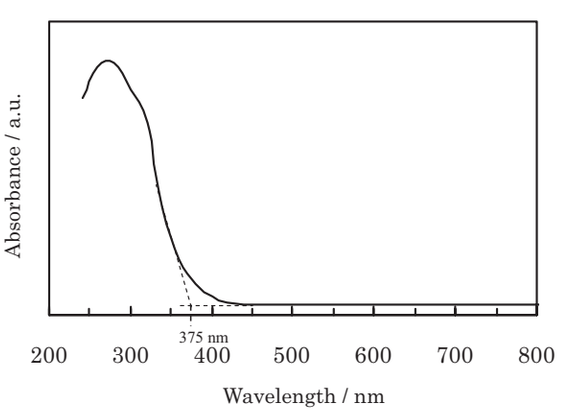

Figure 7. UV-visible spectrum of the TiO_2 thin film on Si/TiO_x/Pt.

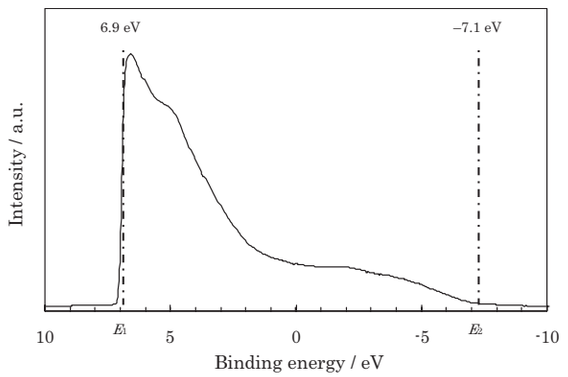

Figure 8. UPS spectrum of $Si/TiO_x/Pt/TiO_2$ measured at the sample bias of −10 V.

E_{bg} = 1240/λ. The value obtained for E_{bg} is considered to be reasonable by comparing with those of the bulk TiO_2 (3.0 eV)[22] and that of the rutile TiO_2 thin film deposited on Si by rf sputtering (3.34 eV).[23,24]

UPS measurements.— Figure 8 shows a typical UPS spectrum of the TiO_2 thin film of the $Si/TiO_x/Pt/TiO_2$ electrode. The spectrum was taken by applying a bias voltage of −10 eV to the sample to enhance the lower emission onset energy (E_1). The ionization potential φ of the TiO_2 thin film was calculated by using the relation $\varphi = h\nu - E_1 + E_2$, where E_2 is the upper emission onset energy and $h\nu$ is the excitation energy of He(I) (21.2 eV). In the spectrum shown in Fig. 8, the photoelectron emission arises at E_1 = 6.9 eV and then decays at E_2 = −7.1 eV. From this result, the ionization potential φ of the TiO_2 thin film, i.e., the energy position of the top of the valence band (E_V) from the vacuum level (E_{vac}), was found to be 7.2 eV.

Figure 9 shows the lower binding energy side of the UPS spectra obtained from two areas of the sample surface: TiO_2 of $Si/TiO_x/Pt/TiO_2$ and Au deposited on a part of $Si/TiO_x/Pt/TiO_2$. The E_F of TiO_2 is at the same position as that of Au deposited on TiO_2, which allows the E_F to be determined. The figure shows the scale of the binding energy with the E_F of Au set at 0 eV. The onset energy of the spectrum, which is estimated to be 2.9 eV, can be attributed to photoelectrons from the position of the E_V of TiO_2. From these results, the E_F of the TiO_2 thin film is consequently located at 4.3 eV below the E_{vac}. Furthermore, we estimate the position of the bottom of the conduction band (E_C) for the TiO_2 thin film as 3.9 eV from the E_{vac} by measuring the E_{bg} value of 3.3 eV and the E_V value of 7.2 eV from the E_{vac}.

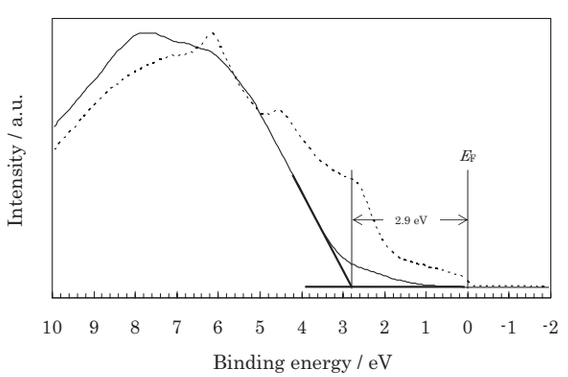

Figure 9. UPS spectra of $Si/TiO_x/Pt/TiO_2$ (solid line) and Au on $Si/TiO_x/Pt/TiO_2$ (dashed line).

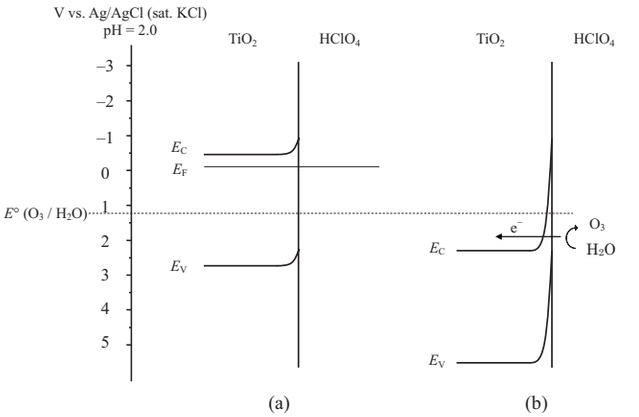

Figure 10. Band models for the $TiO_2/HClO_4$ interface in 0.01 M $HClO_4$ under (a) no anodic/cathodic bias and (b) a large anodic bias.

It is reported that the E_C of many n-type semiconductors is 0.1–0.4 eV more negative than E_F.[25,26] Therefore, the obtained difference (0.4 eV) between the E_F and E_C values is reasonable. The relationship between the absolute electrode potential of an electrode (E_{abs}) and the standard electrode potential (SHE, $E°$) is known as $E_{abs} = E° + 4.44$,[27] and the electrode potential changes at a rate of −0.059 V/pH.[28] In addition, the potential of Ag/AgCl (sat KCl) is taken as 0.199 V vs SHE. Therefore, the values of E_C and E_V of the TiO_2 thin film in 0.01 M $HClO_4$ (pH 2.0) are calculated to be −0.86 and 2.44 V vs Ag/AgCl (sat KCl), respectively. The values obtained for the E_C, E_V, and E_F of the TiO_2 thin film are somewhat different from the reported values.[29-31] This difference may arise from the influence of surface contamination resulting from the ex situ preparation process of the TiO_2 thin film or may be caused by different measurement methods.

Figure 10 shows a schematic illustration of the band structure of the $TiO_2/HClO_4$ interface of the present electrode. When the n-type semiconductor TiO_2 is in contact with the electrolyte solution, a thermodynamic equilibration takes place at the interface,[31] as shown in Fig. 10a. This may result in the formation of a depletion layer within a thin surface region of the TiO_2, in which the electronic energy bands are generally bent toward a higher energy. This layer can be formed by the adsorption of ions and/or molecules in the solution. The counter charges in the semiconductor are not only located at the interface but are also distributed over a finite distance below the surface. Figure 10b shows the case of a large anodic bias applied at the semiconductor/electrolyte interface. At the interface between a semiconductor and an electrolyte, a double layer of charge exists. In such a large anodic bias, the depletion layer would be thin enough for electron transfer from the electrolyte to the conduction band to take place. Therefore, the surface state bringing about a tunneling current[32,33] due to the OER and, furthermore, the EOP can exist at high potential states. We previously discussed a similar concept for the EOP using $Si/TiO_x/Pt/TaO_x$ electrodes,[14] in which it was considered that (*i*) electrons tunnel through the depletion layer and (*ii*) electrons hop along the interfacial levels in the depletion layer. In both cases, the electron transfer occurs at a higher potential than the oxidation–reduction potentials of oxygen and ozone (≧1.51 V vs SHE). As a result, the OER and/or EOP can occur. From the results shown in Fig. 2 and the above-mentioned water oxidation via electron tunneling, the $Si/TiO_x/Pt/TiO_2$ electrode fabricated in this study is highly efficient for EOP probably because of its high oxygen overpotential, compared with the conventional electrodes previously used for EOP. That is, the observed high efficiency of EOP is considered to originate from the electrocatalysis of n-type TiO_2 in the dark when a large anodic bias is applied, in which according to the n-type TiO_2 band structure, a majority carrier (electron) tunneling can take place through a deep

depletion layer of the TiO_2 surface. Therefore, the high EOP efficiency (typically 9% at 8.9 mA cm^{-2}) was achieved using the electrodes completely covered with an n-type TiO_2 thin film. A similar high EOP efficiency was also achieved (8% at 10 mA cm^{-2}) using $Si/TiO_x/Pt/TaO_x$ fabricated in such a way that the Pt substrate is completely covered with a sputtered TaO_x layer,[13] while in the case of the $Si/TiO_x/Pt/TiO_x$ electrode in which the Pt substrate as well as the TiO_x layer were found to function as an electrode surface because of the partial exposure of the Pt substrate to the electrolyte solution, the EOP efficiency was 1.5–4.2% at 16–800 mA cm^{-2}.[15,16] The complete covering of the Pt substrate with the n-type TiO_2 thin film is considered a key factor in achieving the high EOP efficiency at the $Si/TiO_x/Pt/TiO_2$ electrode.

Conclusions

An electrode for EOP with a TiO_2 thin film was fabricated by sputtering it on a $Si/TiO_x/Pt$ substrate. From the electrochemical measurements, this substrate was confirmed to be completely covered with a uniform and dense TiO_2 thin film (its thickness is typically 300 nm), which can function as an active surface for EOP. The fabricated film was found to be of rutile-type TiO_2 and n-type semiconductor by the photoelectrochemical and XRD measurements. The band positions of the TiO_2 thin film were also determined by UPS and UV-visible spectroscopy. The EOP current efficiency of ca. 8% was achieved in the current density range of 8.9–53.3 mA cm^{-2} in 0.01 M $HClO_4$ at 15°C. This high efficiency, in a sense reflecting the high oxygen overpotential of the TiO_2 film (in other words, its electrocatalysis for EOP), originates from the complete covering of the Pt substrate with the n-type TiO_2 thin film.

Acknowledgments

The authors thank Dr. Tsutomu Minegishi, Associate Professor Jun Kubota, and Professor Kazunari Domen at the University of Tokyo for their helpful discussions and skillful assistance in the photoelectrochemical measurements. YA-MAN Ltd. is also acknowledged for the UV-visible spectra measurements.

Tokyo Institute of Technology assisted in meeting the publication costs of this article.

References

1. M. H. P. Santana, L. A. De Faria, and J. F. C. Boodts, *Electrochim. Acta*, **49**, 1925 (2004).
2. M. H. Miles, E. A. Klaus, B. P. Gunn, J. R. Locker, and W. E. Serafin, *Electrochim. Acta*, **23**, 521 (1978).
3. S. Trasatti, *Int. J. Hydrogen Energy*, **20**, 835 (1995).
4. P. C. Foller and C. W. Tobias, *J. Electrochem. Soc.*, **129**, 506 (1982).
5. L. M. Da Silva, L. A. De Faria, and J. F. C. Boodts, *Pure Appl. Chem.*, **73**, 1871 (2001).
6. L. M. Da Silva, L. A. De Faria, and J. F. C. Boodts, *Electrochim. Acta*, **48**, 699 (2003).
7. R. Amadelli, A. De Battisti, D. V. Girenko, S. V. Kovalyov, and A. B. Velichenko, *Electrochim. Acta*, **46**, 341 (2000).
8. K. Arihara, C. Terashima, and A. Fujishima, *J. Electrochem. Soc.*, **154**, E71 (2007).
9. A. Kraft, M. Stadelmann, M. Wunsche, and M. Blaschke, *Electrochem. Commun.*, **8**, 883 (2006).
10. K. Kaneda, M. Ikematsu, Y. Koizumi, H. Minoshima, T. Rakuma, D. Takaoka, and M. Yasuda, *Electrochem. Solid-State Lett.*, **8**, J13 (2005).
11. M. I. Awad, S. Sata, K. Kaneda, M. Ikematsu, T. Okajima, and T. Ohsaka, *Electrochem. Commun.*, **8**, 1263 (2006).
12. K. Kaneda, M. Ikematsu, M. Iseki, D. Takaoka, T. Higuchi, T. Hattori, T. Tsukamoto, and M. Yasuda, *Jpn. J. Appl. Phys., Part 1*, **45**, 5154 (2006).
13. K. Kaneda, M. Ikematsu, M. Iseki, D. Takaoka, T. Higuchi, T. Hattori, T. Tsukamoto, and M. Yasuda, *Chem. Lett.*, **34**, 1320 (2005).
14. K. Kaneda, M. Ikematsu, K. Kitsuka, M. Iseki, H. Matsuura, T. Higuchi, T. Hattori, T. Tsukamoto, and M. Yasuda, *Jpn. J. Appl. Phys., Part 1*, **45**, 6417 (2006).
15. A. M. Mohammad, K. Kitsuka, K. Kaneda, M. I. Awad, A. M. Abdullah, M. Ikematsu, and T. Ohsaka, *Chem. Lett.*, **36**, 1046 (2007).
16. A. M. Mohammad, K. Kitsuka, A. M. Abdullah, M. I. Awad, T. Okajima, K. Kaneda, M. Ikematsu, and T. Ohsaka, *Appl. Surf. Sci.*, **255**, 8458 (2009).
17. K. Kitsuka, K. Kaneda, M. Ikematsu, M. Iseki, K. Mushiake, A. M. Mohammad, and T. Ohsaka, *Chem. Lett.*, **36**, 806 (2007).
18. J. C. G. Thanos, H. P. Fritz, and D. Wabner, *J. Appl. Electrochem.*, **14**, 389 (1984).
19. A. Ishikawa, T. Takata, J. N. Kondo, M. Hara, and K. Domen, *J. Phys. Chem. B*, **108**, 11049 (2004).
20. R. J. Swope, J. R. Smyth, and A. C. Larson, *Am. Mineral.*, **80**, 448 (1995).
21. H. E. Swanson and E. Tatge, *Natl. Bur. Stand. Circ. (U. S.)*, **539**, 28 (1953).
22. O. Diwald, T. L. Thompson, T. Zubkov, E. G. Goralski, S. D. Walck, and J. T. Yates, *J. Phys. Chem. B*, **108**, 6004 (2004).
23. S. Tanemura, L. Miao, P. Jin, K. Kaneko, A. Terai, and N. Nabatova-Gabain, *Appl. Surf. Sci.*, **212–213**, 654 (2003).
24. L. Miao, P. Jin, K. Kaneko, A. Terai, N. Nabatova-Gabain, and S. Tanemura, *Appl. Surf. Sci.*, **212–213**, 255 (2003).
25. Y. Matsumoto, M. Omae, I. Watanabe, and E. Sato, *J. Electrochem. Soc.*, **133**, 711 (1986).
26. Y. Matsumoto, *J. Solid State Chem.*, **126**, 227 (1996).
27. S. Trasatti, *Pure Appl. Chem.*, **58**, 955 (1986).
28. N. Chandrasekharan and P. V. Kamat, *J. Phys. Chem. B*, **104**, 10851 (2000).
29. K. D. Schierbaum, S. Fischer, M. C. Torquemada, J. L. deSegovia, E. Roman, and J. A. MartinGago, *Surf. Sci.*, **345**, 261 (1996).
30. J. Ivanco, T. Haber, J. R. Krenn, F. P. Netzer, R. Resel, and M. G. Ramsey, *Surf. Sci.*, **601**, 178 (2007).
31. A. J. Nozik and R. Memming, *J. Phys. Chem.*, **100**, 13061 (1996).
32. P. J. Boddy, *J. Electrochem. Soc.*, **115**, 199 (1968).
33. Y. Matsumoto, T. Sasaki, and J. Hombo, *J. Electrochem. Soc.*, **138**, 1259 (1991).